Supporting information for: Charge Carrier Trapping at Surface Defects of Perovskite Solar Cell Absorbers: A First-Principles Study

Hiroki Uratani*,†,‡ and Koichi Yamashita*,†,‡

†*Department of Chemical System Engineering, School of Engineering, The University of Tokyo, 7-3-1, Hongo, Bunkyo-ku, 113-8656 Tokyo, Japan*

‡*CREST-JST, 7 Gobancho, Chiyoda-ku, 102-0076 Tokyo, Japan*

E-mail: uratani@tcl.t.u-tokyo.ac.jp; yamasita@chemsys.t.u-tokyo.ac.jp

1 Determination of the Kohn-Sham states associated with VBM, CBM, and defect states.

The Kohn-Sham states associated with the VBM, CBM, and defect states are determined by their (i) absolute energy levels: the VBM and CBM of defect-containing systems must be located near those of non-defect-containing systems, (ii) occupation numbers: for p-type defects, the defect states or VBM must be unoccupied, and for n-type defects, the defect states or CBM must be occupied, and (iii) orbital shapes: the Kohn-Sham orbitals corresponding to the defect states must be localized. The orbital energy levels, occupation numbers, and orbital shapes (charge density distribution derived from the orbitals) of considered systems calculated by HSE ($a = 0.43$) with SOC are shown in Figure S1-S16. The orbital energy levels are referenced to calculated vacuum level of each system. The occupation numbers are assigned by the Gaussian smearing method, which is a conventional technique for periodic DFT calculations. In this method, the occupation number f is determined by the function

$$f = \frac{1}{2}\left(1 - \mathrm{erf}\left[\frac{\epsilon - \mu}{\sigma}\right]\right), \tag{1}$$

where ϵ is the orbital energy and μ is the Fermi level. The parameter σ was set to be 0.05 eV. The orbital shapes are shown as yellow isosurfaces. Note that the blue isosurfaces indicates unphysical negative charge density, which is a common artifact originating in the PAW method.

MAI

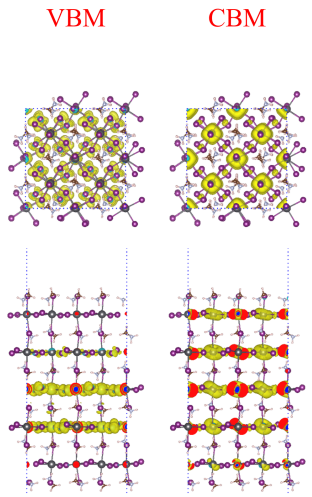

	VBM	CBM
#	2176	2177
Energy (eV)	-4.98	-3.09
Occupation number	1.00	0.00

Figure S1: "MAI" surface.

MAI V_I

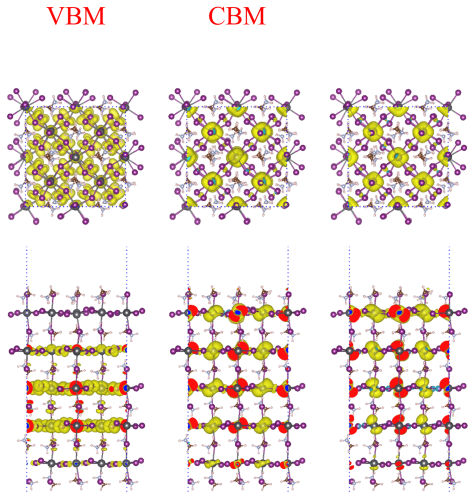

	VBM	CBM	
#	2168	2169	2170
Energy (eV)	-4.72	-2.89	-2.89
Occupation number	1.00	0.50	0.50

Figure S2: V_I on "MAI" surface.

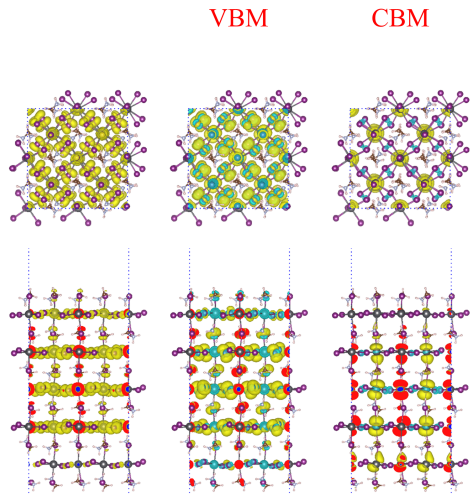

#	2161	2162	2163
Energy (eV)	-4.74	-4.74	-2.89
Occupation number	0.80	0.20	0.00

Figure S3: V_{MA} on "MAI" surface.

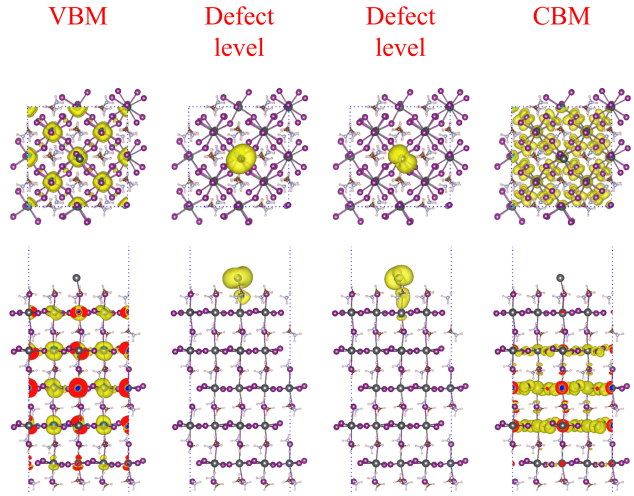

#	2188	2189	2190	2191
Energy (eV)	-5.03	-3.81	-3.76	-3.12
Occupation number	1.00	1.00	1.00	0.00

Figure S4: Pb_i on "MAI" surface.

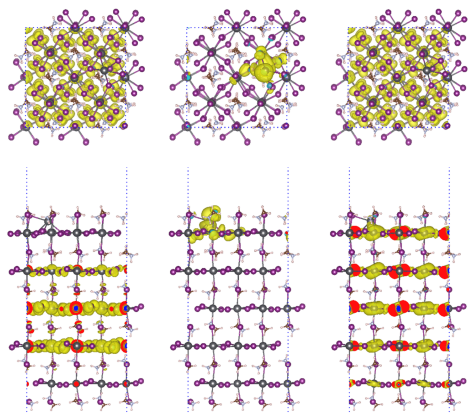

#	2174	2175	2176
Energy (eV)	-4.99	-4.07	-3.10
Occupation number	1.00	1.00	0.00

Figure S5: Pb_{MA} on "MAI" surface.

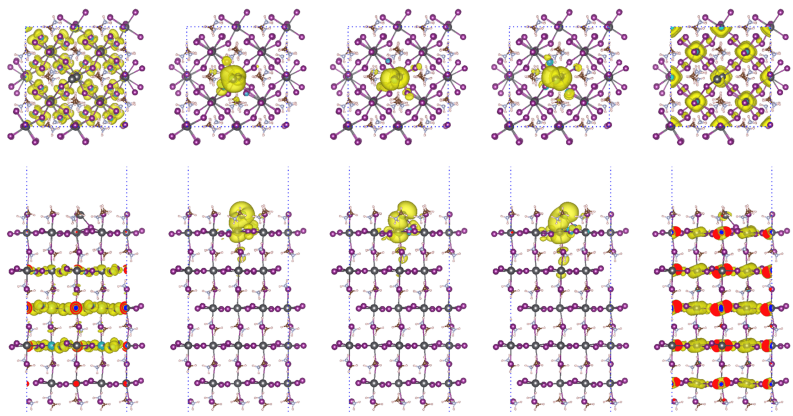

#	2180	2181	2182	2183	2184
Energy (eV)	-4.89	-4.44	-4.29	-3.75	-2.99
Occupation number	1.00	1.00	1.00	1.00	0.00

Figure S6: Pb_I on "MAI" surface.

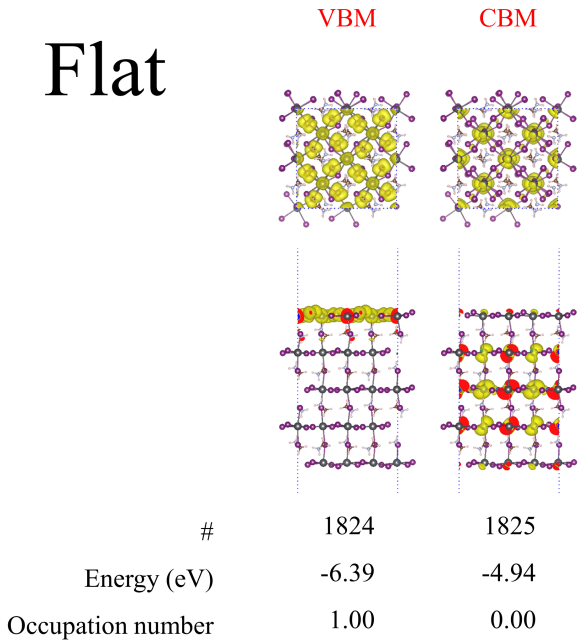

Figure S7: "Flat" surface.

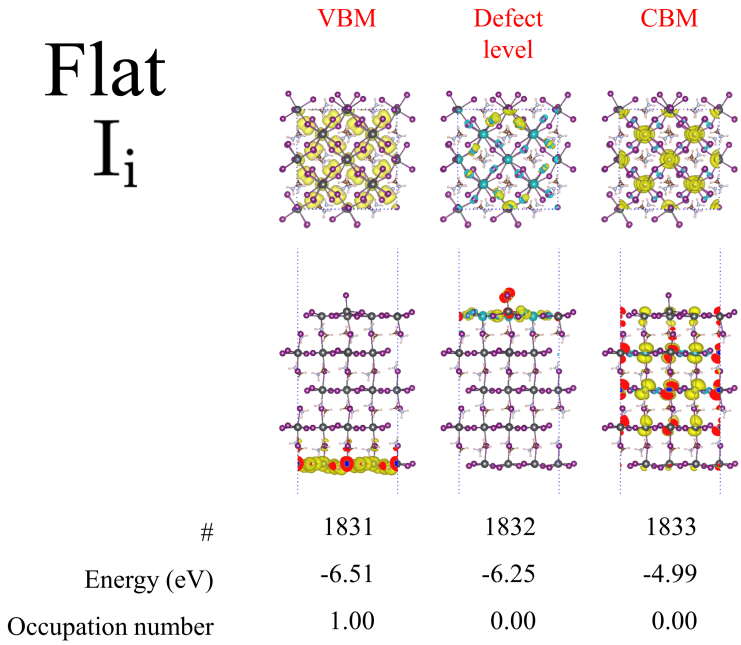

Figure S8: I_i on "flat" surface.

Flat V_I

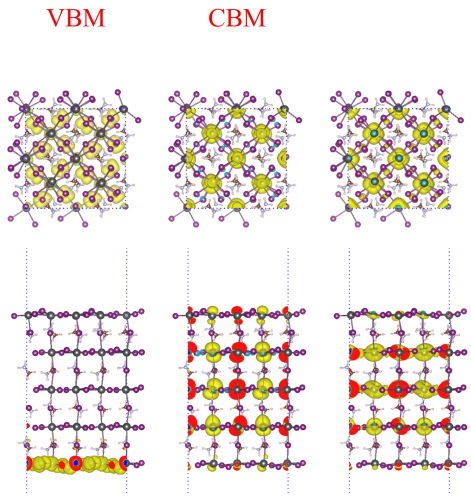

#	1816	1817	1818
Energy (eV)	-6.26	-4.71	-4.71
Occupation number	1.00	0.50	0.50

Figure S9: V_I on "flat" surface.

Flat Pb_i

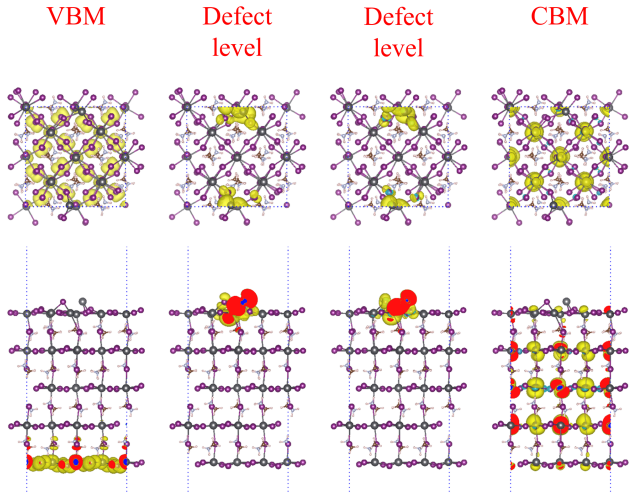

#	1836	1837	1838	1839
Energy (eV)	-6.52	-5.66	-5.66	-4.90
Occupation number	1.00	1.00	1.00	0.00

Figure S10: Pb_i on "flat" surface.

Flat
V_{Pb}

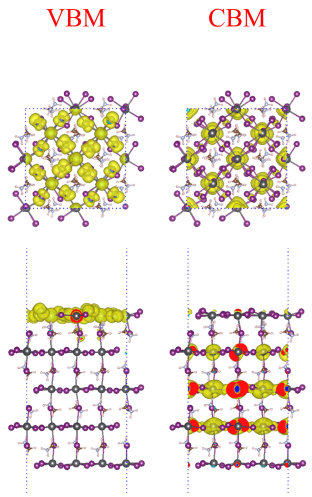

	VBM	CBM
#	1812	1813
Energy (eV)	-6.29	-4.90
Occupation number	0.00	0.00

Figure S11: V_{Pb} on "flat" surface.

Vacant

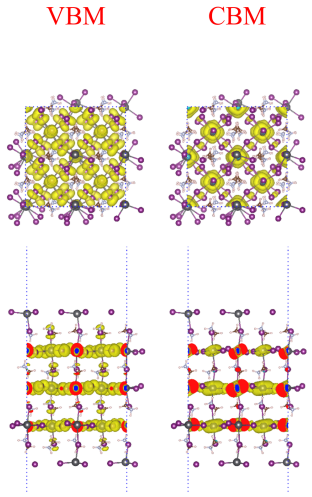

	VBM	CBM
#	1600	1601
Energy (eV)	-6.18	-4.24
Occupation number	1.00	0.00

Figure S12: "Vacant" surface.

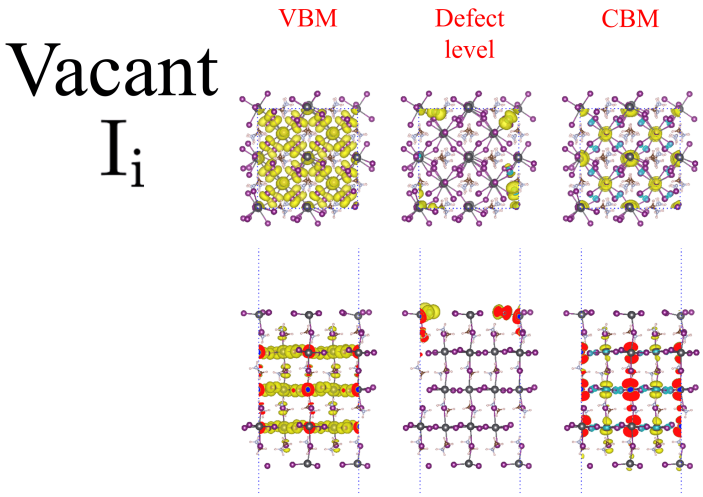

#	1607	1608	1609
Energy (eV)	-6.08	-5.15	-4.13
Occupation number	1.00	0.00	0.00

Figure S13: I_i on "vacant" surface.

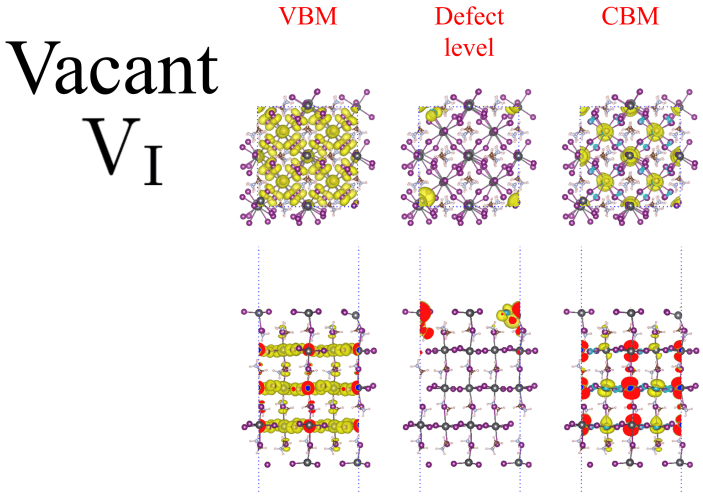

#	1592	1593	1594
Energy (eV)	-6.01	-4.91	-4.03
Occupation number	1.00	1.00	0.00

Figure S14: V_I on "vacant" surface.

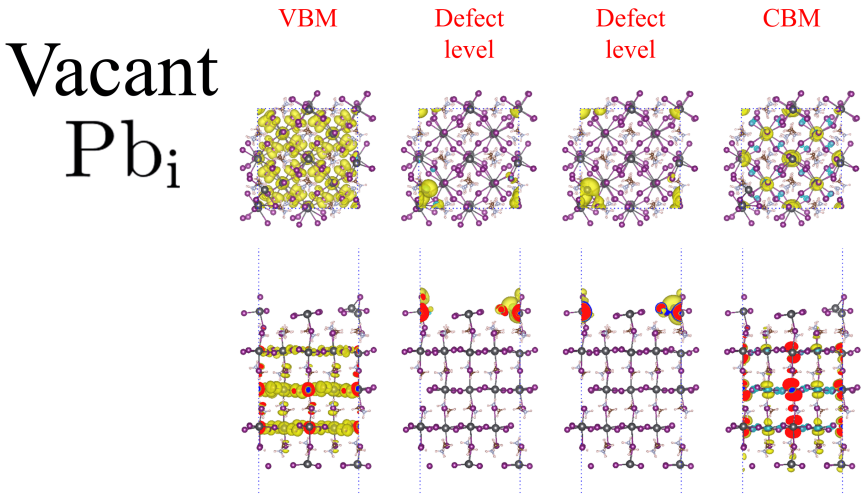

#	1612	1613	1614	1615
Energy (eV)	-6.15	-5.09	-5.09	-4.10
Occupation number	1.00	1.00	1.00	0.00

Figure S15: Pb_i on "vacant" surface.

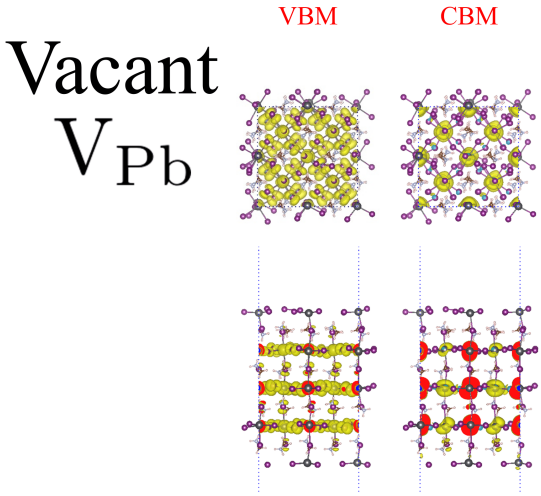

#	1586	1587
Energy (eV)	-6.04	-4.03
Occupation number	1.00	0.00

Figure S16: V_{Pb} on "vacant" surface.

2 Defect formation energy calculations.

The defect formation energy was calculated following the strategy of Yin et al.[S1] Here, μ_{I}, μ_{Pb}, and μ_{MA} are the chemical potential of I, Pb, and MA, respectively, referenced to the state of I_2(g), Pb(s), and MA(s) summarized in Table SI, respectively. The calculations were conducted with GGA-PBE functional without the inclusion of spin-orbit coupling, 500 eV of a plane-wave cutoff, and a convergent k-point mesh. The structures were relaxed until the Hellmann-Feynman force become below 0.005 eV / Å. We define ΔH_1, ΔH_2, and ΔH_3

Table SI: Calculated total energy of each species. a:bcc phase, following Cs.[S1] b: Rock-salt phase.[S1,S2] c: Tetragonal phase.

Species	Total energy (eV)
I_2(g)	-2.65
Pb(s)	-3.56
MA(s)[a]	-37.75
MAI(s)[b]	-42.23
PbI_2(s)	-8.62
$MAPbI_3$(s)[c]	-50.89

as the change in enthalpy corresponding to the reactions

$$\mathrm{MA(s)} + \mathrm{Pb(s)} + \frac{3}{2}\mathrm{I_2(g)} \rightarrow \mathrm{MAPbI_3(s)}, \tag{2}$$

$$\mathrm{MA(s)} + \frac{1}{2}\mathrm{I_2(g)} \rightarrow \mathrm{MAI(s)}, \tag{3}$$

$$\mathrm{Pb(s)} + \mathrm{I_2(g)} \rightarrow \mathrm{PbI_2(s)}, \tag{4}$$

respectively. Hence, $\Delta H_1 = -5.60\,\mathrm{eV}$, $\Delta H_2 = -3.15\,\mathrm{eV}$, and $\Delta H_3 = -2.41\,\mathrm{eV}$. Assuming equilibrium among MAI, PbI_2, and $MAPbI_3$, μ_I, μ_Pb, and μ_MA must satisfy

$$\mu_\mathrm{MA} + \mu_\mathrm{Pb} + 3\mu_\mathrm{I} = \Delta H_1 = -5.60\,\mathrm{eV}, \tag{5}$$

$$\mu_\mathrm{MA} + \mu_\mathrm{I} < \Delta H_2 = -3.15\,\mathrm{eV}, \tag{6}$$

$$\mu_\mathrm{Pb} + 2\mu_\mathrm{I} < \Delta H_3 = -2.41\,\mathrm{eV}, \tag{7}$$

$$\mu_\mathrm{MA}, \quad \mu_\mathrm{Pb}, \quad \mu_\mathrm{I} < 0. \tag{8}$$

The range of (μ_Pb, μ_I) which can satisfy Eqs. 5-8 is shown by red area in Figure S17 and consistent with previous works.[S1,S3] The points A, B, and C in Figure S17 correspond to the I-rich, moderate, and Pb-rich condition in the main text, respectively. The defect formation

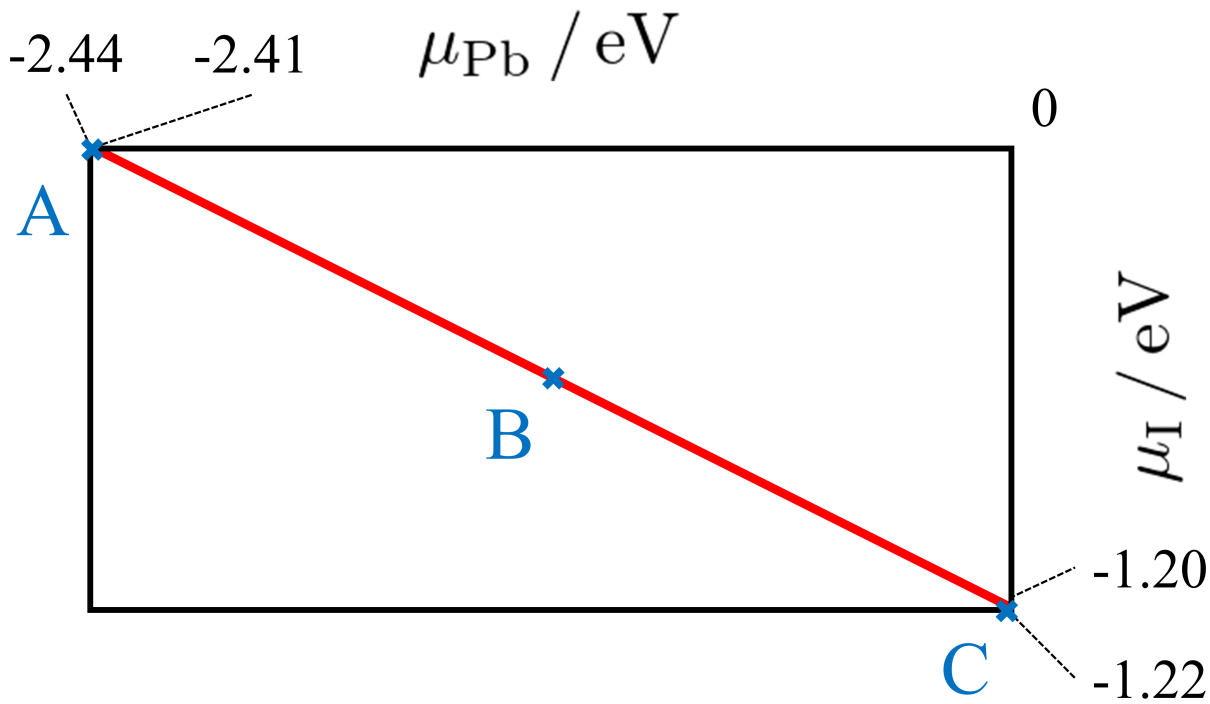

Figure S17: The range of (μ_Pb, μ_I) which can satisfy Eqs. 5-8 (red area). A, B, and C are the I-rich condition ($\mu_\mathrm{I} = 0\,\mathrm{eV}$, $\mu_\mathrm{Pb} = -2.44\,\mathrm{eV}$, and $\mu_\mathrm{MA} = -3.15\,\mathrm{eV}$), the moderate condition ($\mu_\mathrm{I} = -0.61\,\mathrm{eV}$, $\mu_\mathrm{Pb} = -1.21\,\mathrm{eV}$, and $\mu_\mathrm{MA} = -2.57\,\mathrm{eV}$), and the Pb-rich condition ($\mu_\mathrm{I} = -1.22\,\mathrm{eV}$, $\mu_\mathrm{Pb} = 0\,\mathrm{eV}$, and $\mu_\mathrm{MA} = -1.93\,\mathrm{eV}$), respectively.

energy is calculated as

$$E_{\mathrm{defect}} - \left(E_{\mathrm{non-defect}} + \Delta n_{\mathrm{I}} \left[\mu_{\mathrm{I}} + \frac{1}{2} E_{\mathrm{I}_2} \right] + \Delta n_{\mathrm{Pb}} \left[\mu_{\mathrm{Pb}} + E_{\mathrm{Pb}} \right] + \Delta n_{\mathrm{MA}} \left[\mu_{\mathrm{MA}} + E_{\mathrm{MA}} \right] \right). \quad (9)$$

E_{defect} is calculated total energy of the defect-containing system, and $E_{\mathrm{non-defect}}$ is that of the non-defect-containing system, i.e. "MAI", "flat", or "vacant" termination without defects. Δn_{I}, Δn_{Pb}, and Δn_{MA} are the change in number of I, Pb, and MA associated with the defect formation, respectively. E_{I_2}, E_{Pb}, and E_{MA} are calculated total energy of I_2(g), Pb(s), and MA(s) summarized in Table SI, respectively.

References

(S1) Yin, W.-J.; Shi, T.; Yan, Y. Unusual defect physics in $CH_3NH_3PbI_3$ perovskite solar cell absorber. *Appl. Phys. Lett.* **2014**, *104*, 063903/1–063903/4.

(S2) Hendricks, S. B. The crystal structures of the monomethyl ammonium halides. *Z. Kristallogr.* **1928**, *67*, 106–118.

(S3) Haruyama, J.; Sodeyama, K.; Han, L.; Tateyama, Y. Termination Dependence of Tetragonal $CH_3NH_3PbI_3$ Surfaces for Perovskite Solar Cells. *J. Phys. Chem. Lett.* **2014**, *5*, 2903–2909.